# Simulation of Spatially Correlated Ground Motion Records Using Stochastic Point-Source Model


**T.J. Liu & H.P. Hong**
*Department of Civil and Environmental Engineering, University of Western Ontario, Canada N6A 5B9*

**SUMMARY:**
Ground motions from an earthquake are spatially correlated. This correlation can be important to assess the seismic hazard and risk for a spatially distributed infrastructure or a group of buildings in a region. The available stochastic models that match the peak ground motions and response spectra well for given earthquake scenario are valuable tools for seismic hazard and risk assessment, although they fail to reproduce the observed spatial correlation characteristics. The present study incorporates the coherency function in the stochastic point-source ground-motion simulation program to sample the ground motion records. It is shown that the strong ground motion records simulated from the proposed procedure can lead to the spatial correlations of the peak ground acceleration and of the spectral accelerations that resemble those observed from the actual records.

*Keywords: spatial correlation; coherency; stochastic point-source method.*

## 1. INTRODUCTION

The ground motions for a given seismic event are spatially correlated. This correlation is measured in terms of the coherency function (Harichandran and Vanmarcke, 1986; Hao *et al*., 1989; Der Kiureghian, 1996; Zerva, 2009), or the intraevent (i.e., station to station) spatial correlation of ground motion parameters, such as peak ground acceleration (PGA) and spectral accelerations (SAs) (Boore *et al.*, 2003; Kawakami and Mogi, 2003; Wang and Takada, 2005; Goda and Hong, 2008a; Jayaram and Baker, 2009; Goda and Atkinson, 2009, 2010).

The coherency function between two ground acceleration time histories recorded at two stations for a given seismic event represents the correlation of two signals at different frequencies and inter-station separation distance. Evaluation and modeling of spatial coherency have been carried out based on the recordings from dense arrays such as the El Centro differential array (Bycroft, 1980) in California, the SMART-1 array (Bolt *et al*., 1982) and the LSST array (Abrahamson *et al*., 1991) in Taiwan. Coherency models has been proposed and used in the analysis of responses of multiple-support structures (Zerva, 1991; Harichandran *et al*., 1996). The models are considered to be applicable for a separation distance less than a few kilometers as the records used to develop and calibrate the models are obtained within a few kilometers. In contrast, the spatial correlation models of PGA and of SAs (Boore *et al.*, 2003 Goda and Hong, 2008a; Jayaram and Baker, 2009) are developed for a separation distance for about up to 50 km (and beyond this distance the correlation can be ignored).

The correlation can affect the probabilistic characteristics of the seismic response and risk for a single spatially distributed infrastructure (such as pipeline or power transmission systems), or a group of buildings distributed in a region (Goda and Hong, 2008b). For regions without enough empirical data (i.e., ground motion records), stochastic ground motion simulation methods such as the stochastic point-source method (Boore, 2003) and the stochastic finite-fault method (Motazedian and Atkinson, 2005) have been used to generate synthetic records to carry out seismic hazard/risk analysis (Atkinson and Boore, 2006). Moreover, the stochastic point-source method and the stochastic finite-fault method

are widely used ground motion simulation techniques that have been proved to be simple and effective in the generation of synthetic ground-motion records (Boore, 1983, 2003 and 2009; Motazedian and Atkinson, 2005; Atkinson *et al*., 2009). The results obtained from these methods matches ground motion measures observed in earthquakes over a broad frequency range. However, it was shown that the stochastic finite-fault method fails to reproduce the observed intraevent spatial correlation characteristics of peak ground motion parameters (i.e., PGA and SAs) (Liu *et al*., 2012).

In this study, it is shown that the stochastic point-source method, similar to the stochastic finite-fault method, fails to reproduce the observed spatial correlation characteristics of peak ground motion measures such as the PGA and SAs. To enhance the stochastic point-source method for seismic hazard and risk analysis, a procedure to incorporate the coherency into the method is proposed. The procedure basically applies the autoregressive-moving-average (ARMA) method to sample white noises with prescribed coherency function, and uses the sampled time histories in the stochastic point-source model through the time modulation, and frequency modulation leading to coherent ground motion records. The spatial correlation characteristics of the simulations of the proposed procedure are investigated.

## 2. SIMULATION USING STOCHASTIC POINT-SOURCE MODEL

The stochastic point-source method developed by Boore (1983, 2003) is a simple to use method and generates records that match specified Fourier spectrum of shear wave at a distance $R$ (normally hypocentral distance) from a fault with seismic moment $M_0$, $Y(M_0, R, f)$. $Y(M_0, R, f)$ is given by,

$$Y(M_0, R, f) = E(M_0, f)P(R, f)G(f)I(f), \tag{2.1}$$

where $f$ is the frequency in Hz; $E(M_0, f)$, $P(R, f)$ and $G(f)$, which are shown in Table 1, represent the impacts from source, path and site, respectively; $M_0$ is related to the moment magnitude (see Table 1); $I(f)$ is an indicator for ground motion type (acceleration, velocity or displacement). The steps to sample ground motions with the stochastic point-source method are summarized below (Boore, 2003):
1) Sample Gaussian noise (signal or time history) with zero mean and unit variance;
2) Modulate the signal using an adopted time modulating function;
3) Transform the windowed signal into frequency domain to obtain its Fourier amplitude spectrum;
4) Normalize the result by the square-root of the mean square amplitude spectrum;
5) Multiply the normalized spectrum to the point source spectrum defined by Eqn. 2.1; and
6) Calculate the synthetic ground motion record by applying the inverse Fourier transform to the spectrum obtained in Step 5).

To test the correlation characteristics of the stochastic point-source model, consider the recording stations that are placed in similar fashion as the SMART-1 array. This is shown in Fig. 1 and the source to array center distance $R_c$ is considered to be equal to 100 km. As indicated in the figure, the test array consists of one center station and 36 stations located in three concentric rings with 12 equally spaced stations for each ring. The radius of the inner ring ($R_{in}$), middle ring ($R_{mid}$) and outer ring ($R_{out}$) are 2.5 km, 12.5 km and 25 km, respectively. A pair of records (at inner ring stations I03 and I04) for $R_c$ = 100 km, **M** = 7.6, are sampled according to the steps described previously and the obtained records are illustrated in Figs. 2(a) and 2(b). For the simulation, the stochastic point-source simulation program was obtained from Boore's personal website (http://daveboore.com/software_online.html, last accessed March 2011), and the parameters adopted for the simulation are listed in Table 2. These parameters are those used by Liu *et al*. (2012) to investigate the spatial correlation of the records generated by the stochastic finite-fault model.

**Table 1**. Summary of stochastic point-source model

| Parameter | Notes |
|---|---|
| Source effect<br>$E(M_0, f) = CM_0 S(M_0, f)$ | $C = \dfrac{\langle R_{\Theta\Phi} \rangle VF}{4\pi\rho_S \beta_S^3 R_0}$ is constant, where $\langle R_{\Theta\Phi} \rangle$ is the radiation pattern; $V = 1/\sqrt{2}$ is the partition of total shear-wave energy into horizontal components; $F = 2$ represents the effect of the free surface; $\rho_S$ and $\beta_S$ are the density and shear-wave velocity in the vicinity of the source, and $R_0 = 1$ km is a reference distance.<br>Seismic moment $M_0$ is given by $\log M_0 = 1.5\mathbf{M} + 16.1$, where **M** is the moment magnitude.<br>$S(M_0, f) = \dfrac{1}{1 + (f / f_0)^2}$ is the $\omega$-square displacement source spectrum. |
| Path effect<br>$P(R, f) = Z(R) \exp\left[\dfrac{-\pi f R}{Q(f) c_Q}\right]$ | $Z(R)$ is the geometrical spreading and $Q(f)$ is the attenuation term. |
| Site effect<br>$G(f) = A(f) D(f)$ | $A(f(z)) = \sqrt{Z_S / \overline{Z}(f)}$ is the amplification term where $Z_S$ and $\overline{Z}(f)$ are the seismic impedance near the source and the near-surface average seismic impedance, respectively.<br>$D(f)$ is the diminution operator, can be the $f_{max}$ filter or the $\kappa_0$ filter. |

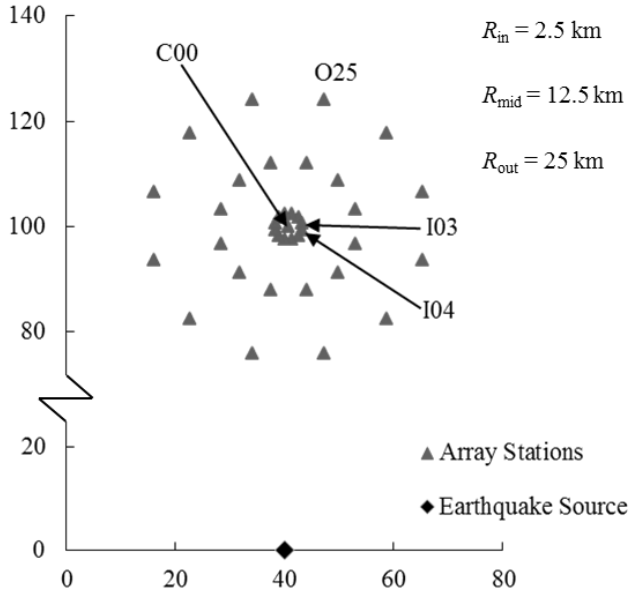


**Figure 1.** Layout of the test array with source to center distance $R_c$ = 100 km.

Using the simulated records shown in Figs. 2(a) and 2(b), the estimated coherency is depicted in Fig. 2(c) showing that the records are incoherent even at such close locations (i.e., separation distance $\Delta$ = 1.3 km), which is expected. For the evaluation of the coherency, we note that the unsmoothed lagged coherency estimate for a pair of records would identically equal to unity (Zerva 2009). Smoothing procedure using a window function not only reduces the variance of the spectral estimations, also extracts the coherency information from the signals. Hamming window is one of the most commonly used window functions given by:

$$W(m) = 0.54 - 0.46\cos\left(\frac{\pi(m+M)}{M}\right) \qquad m = -M, ..., M\,, \tag{2.2}$$

where $M$ is a parameter and the window width is given by $2M + 1$. $M = 5$ for time series less than approximately 2000 samples has been suggested (Abrahamson *et al*. 1991). Number of samples for a record component can be significant larger because of the high sampling frequency of modern instrument (accelerograph) or the long excitation duration of large earthquakes. A wider Hamming spectral window seems appropriate in such cases to yield smooth spectral estimates. For the estimates shown in Fig. 2(c) $M$ equal to 300 is considered.

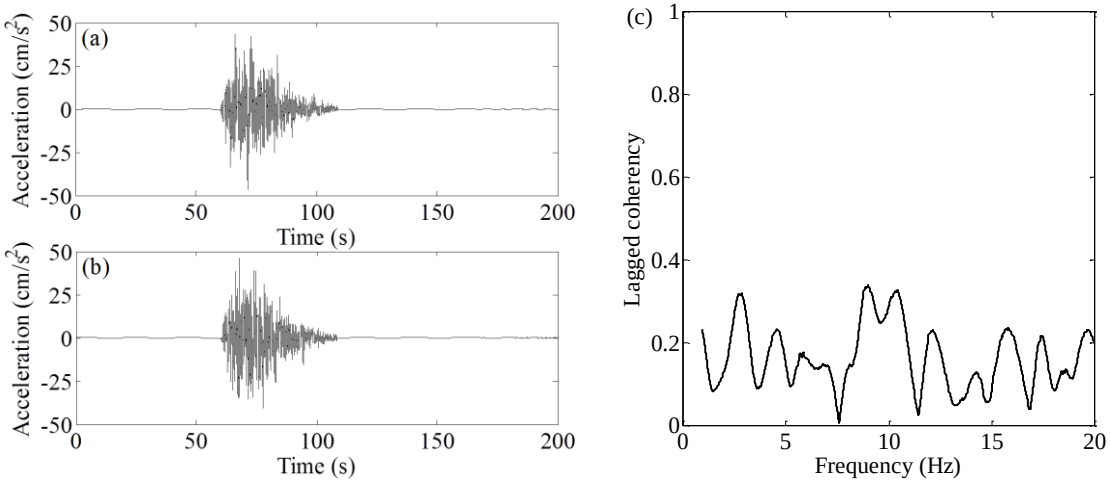


**Figure 2.** Sampled records for $R_c$ = 100 km, **M** = 7.6, and estimated coherency function.

The analysis leading to Fig. 2 was repeated for different pairs of stations, confirming the records obtained from the stochastic point-source model are incoherent. Also, the correlation coefficient of the PGA and of the SA values for the paired records from repeated analyses are calculated, again as expected, they are near zero. This observation differs from the one given in Liu *et al*. (2012), showing that the correlation coefficient for the stochastic finite-fault method decrease with increased distance. This discrepancy is due to that residuals for the rock and soil sites of stochastic finite-fault simulations are not statistically homogeneous and they should be analysed separately as two sets of data.

**Table 2.** Modeling parameters in stochastic point-source model (Liu *et al*. 2012)

| Parameter | Parameter value |
|---|---|
| Stress parameter Δσ (bar) | 100 |
| $Q(f)$ | $117 \cdot f^{0.77}$ |
| Geometrical spreading | $1/R$ for $R < 50$ km<br>$1/R^0$ for 50 km $\leq R <$ 150 km<br>$1/R^{0.5}$ for $R \geq$ 150 km |
| Windowing function | Exponential (Saragoni and Hart, 1974) |
| Kappa (s) | 0.06 |
| Crustal amplification | Boore and Joyner (1997) western North America generic rock site |
| Crustal shear-wave velocity (km/s) | 3.2 |
| Crustal density (g/cm$^3$) | 2.7 |

## 3. EXTENDED STOCHASTIC POINT-SOURCE MODEL USING COHERENT WHITE NOISES

To improve the spatial correlation characteristics of the stochastic point-source model, we propose to incorporate the coherency function in the model. Basically, a vector of spatial-coherent white noises

is generated using ARMA model (Samaras *et al*., 1985). The white noises are then fed to the stochastic point-source model to simulate the ground motions at different spatial locations. The simulated ground motion records are records with pre-described coherency function that depends on the distances between the considered recording stations (or sites). The spatial correlation characteristics of the ground motion records simulated using the proposed procedure for an adopted coherency function are also investigated in the following.

### 3.1. Spatially coherent white noises based on ARMA method

Consider that the coherency function of the ground motions for an earthquake event at two stations *j* and *k*, is defined as:

$$\bar{\gamma}(\Delta, f) = \frac{\bar{S}_{jk}(f)}{\sqrt{\bar{S}_{jj}(f)\bar{S}_{kk}(f)}} \tag{3.1}$$

where $\bar{S}_{jk}(f)$ is the smoothed cross spectrum of the acceleration time histories of two randomly selected horizontal ground motion components at the two stations; $\bar{S}_{jj}(f)$ and $\bar{S}_{kk}(f)$ are the corresponding power spectral density functions. The lagged coherency, $\left|\bar{\gamma}(\Delta, f)\right|$, is a measure of "similarity" in the seismic motions, and indicates the degree to which the data recorded at the two stations are related by means of a linear transfer function (Brillinger, 1981).

One of the coherency functions in the literature is proposed by Harichandran and Vanmarcke (1986):

$$\gamma(\Delta, f) = A\exp\left(-\frac{2\Delta}{\alpha\theta(f)}(1-A+\alpha A)\right)+(1-A)\exp\left(-\frac{2\Delta}{\theta(f)}(1-A+\alpha A)\right) \tag{3.2}$$

where $\Delta$ is the separation distance between two locations *j* and *k* in km and $\theta(f) = k\left[1+\left(\frac{f}{f_0}\right)^b\right]^{-\frac{1}{2}}$, in which *f* is the frequency; *A*, $\alpha$, *k*, $f_0$ and *b* are model parameters. Harichandran and Vanmarcke (1986) suggested that the parameters could take the following values $A = 0.736$, $\alpha = 0.147$, $k = 5210$, $f_0 = 1.09$ and $b = 2.78$.

Use of the values suggested by Harichandran and Vanmarcke (1986) and Eqn. 3.2 leads to very small value of the coherency function for $\Delta$ greater than 5 km. This is in contrast with the coherency shown in Fig. 3, which are estimated from the Chi-Chi earthquake records using Hamming window with $M$ = 20. The relatively significant coherency (with average value around 0.3) is also reflected in the significant spatial correlation of the PGA and of the SAs for $\Delta$ greater than 5 km (Goda and Hong, 2008a; Liu *et al*., 2012). Therefore, it is expected that the values of the parameters *A*, $\alpha$, *k*, $f_0$ and *b* need to be modified to increase the spatial coherency if one is interested in reproduce approximately the spatial correlation trends for the PGA and SAs that are observed from large earthquakes.

Given a coherency structure, a vector process of white noises $K(t)$ can be generated using ARMA model (Samaras *et al*., 1985):

$$K(t) = \sum_{i=1}^{q} A_i K(t-i\Delta t) + \sum_{i=1}^{q} B_i \psi(t-i\Delta t) \tag{3.3}$$

where $\psi(t - i\Delta t)$ is the vector of Gaussian white noise and it is assumed that $t$ takes on values $i\Delta t$ where $i$ is an integer; $A_i$ and $B_i$ are the coefficients of autoregressive and moving-average model, respectively; $q$ is the orders of the autoregressive part and of the moving-average part (which is assumed to be the same). $A_i$ and $B_i$ are to be determined based on the assigned spectral and coherency function.

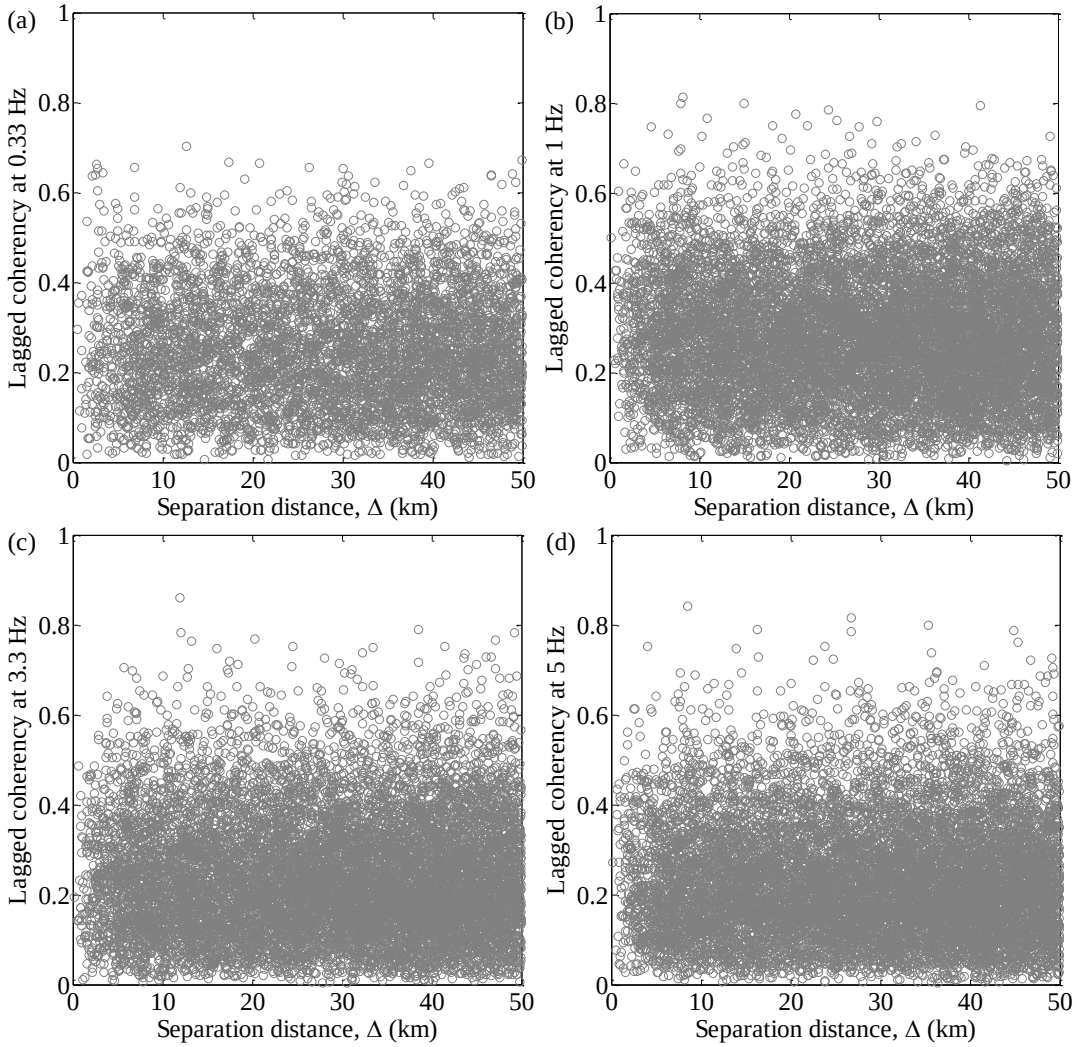


**Figure 3.** Estimated lagged coherency of Chi-Chi records.

### 3.2 Sampled spatially correlated ground motion records

As mentioned earlier, by giving the spatially coherent white noises as the input to the stochastic point-source model, coherent ground motion records at different spatial locations with Fourier spectrum defined in Eqn. 2.1 can be obtained following the procedure summarized in the previous section. For the numerical analysis, we use the coherency functions shown in Eqn. 3.2 with the following parameters $A$ = 0.45, $\alpha$ = 0.05, $k$ = 80000, $f_0$ = 2.0, $b$ = 1.0 and $\Delta$ is 1/10 of the separation distance in meters and the Fourier spectrum with the parameters shown in Table 2 for an earthquake event **M** = 7.6 at $R_c$ = 100 km. We refer this case as the reference case in the following for easy explanation.

First, we sample records at recording stations shown in Fig. 1. We calculate the lagged coherency using Hamming window with $M$ = 200 for both the input coherent white noises and the simulated records at the stations C00 and O25 (see Fig. 1). The estimated coherency are compared to the prescribed coherency function in Fig. 4(a), indicating that coherency for the white noises and for the simulated ground motion records mimics the prescribed function.

We repeat the simulation process 100 times, and estimate the PGA and SAs at each recording station. Using these samples, the spatial correlation coefficients, $\rho(\Delta, T)$, can be calculated using:

$$\rho(\Delta,T) = \frac{E\left[\left(\ln Y_j - \mu_{\ln Y_j}\right)\left(\ln Y_k - \mu_{\ln Y_k}\right)\right]}{\sigma_{\ln Y_j}\sigma_{\ln Y_k}} \tag{3.4}$$

where $Y_j$ and $Y_k$ are the ground motion measures at two stations $j$ and $k$; $\mu_{(\bullet)}$ and $\sigma_{(\bullet)}$ are the mean and standard deviation of the variable; $E(\bullet)$ represents expectation; $T$ is the natural vibration period of the ground motion measures and $\Delta$ is the separation distance. The estimated spatial correlation coefficients of peak ground motions (i.e., SAs) at 0.3 s, 1.0 s and 3.0 s are shown in Fig. 4(b), 4(c) and 4(d), respectively. Also shown in the figure is the fitted empirical spatial correlation coefficient function:

$$\rho(\Delta,T) = \exp\left(-a\Delta^b\right) \tag{3.5}$$

where $a$ and $b$ are the model parameters. Figs. 4(b) to 4(d) indicate that the spatial correlation coefficients for the simulated records decays as separation distance increases. This is consistent with the trends that can be obtained for the actual records from California, Taiwan and Japan (Kawakami and Mogi, 2003; Wang and Takada, 2005; Goda and Hong, 2008a; Jayaram and Baker, 2009; Goda and Atkinson, 2009, 2010). The scatter of the correlation coefficient samples becomes larger for lower coherency value (i.e., for increased separation distance).

### 3.3 Impact of input parameters on spatial correlations

To see how the prescribed coherency function, the magnitude, and the source distance $R_c$ impact the spatial correlation of the simulated records, we consider three additional three cases by maintenance the parameters same as those of reference case except that: for Case 1 the prescribed coherency function is defined by the parameters $A$ = 0.6, $\alpha$ = 0.05, $k$ = 60000, $f_0$ = 0.5 and $b$ = 2.0, as shown in Fig. 5; for Case 2 **M** =7, and for Case 3 $R_c$ = 50 km. Again, the simulation is carried out and a simulation cycle of 100 for each case that is considered. The estimated mean values of the spatial correlation coefficients of PGA and SAs at 0.3 s, 1.0 s and 3.0 s are compared to that of the reference case in Fig. 6. The figure shows that lowering the coherency (Case 1) leads to decreased spatial correlation, which is expected. The impact of earthquake magnitude and source distance parameters on the spatial correlations is insignificant since the differences between the spatial correlations for the reference case, Case 2 and Case 3 are not significant. Whether this observation can be made from the historical ground motion records are unknown at present. Moreover, a further scrutiny of the proposed procedure to simulate coherent records may be required as it was observed that the needed coherency to reproduce the observed spatial correlation seems to be higher than those observed from records.

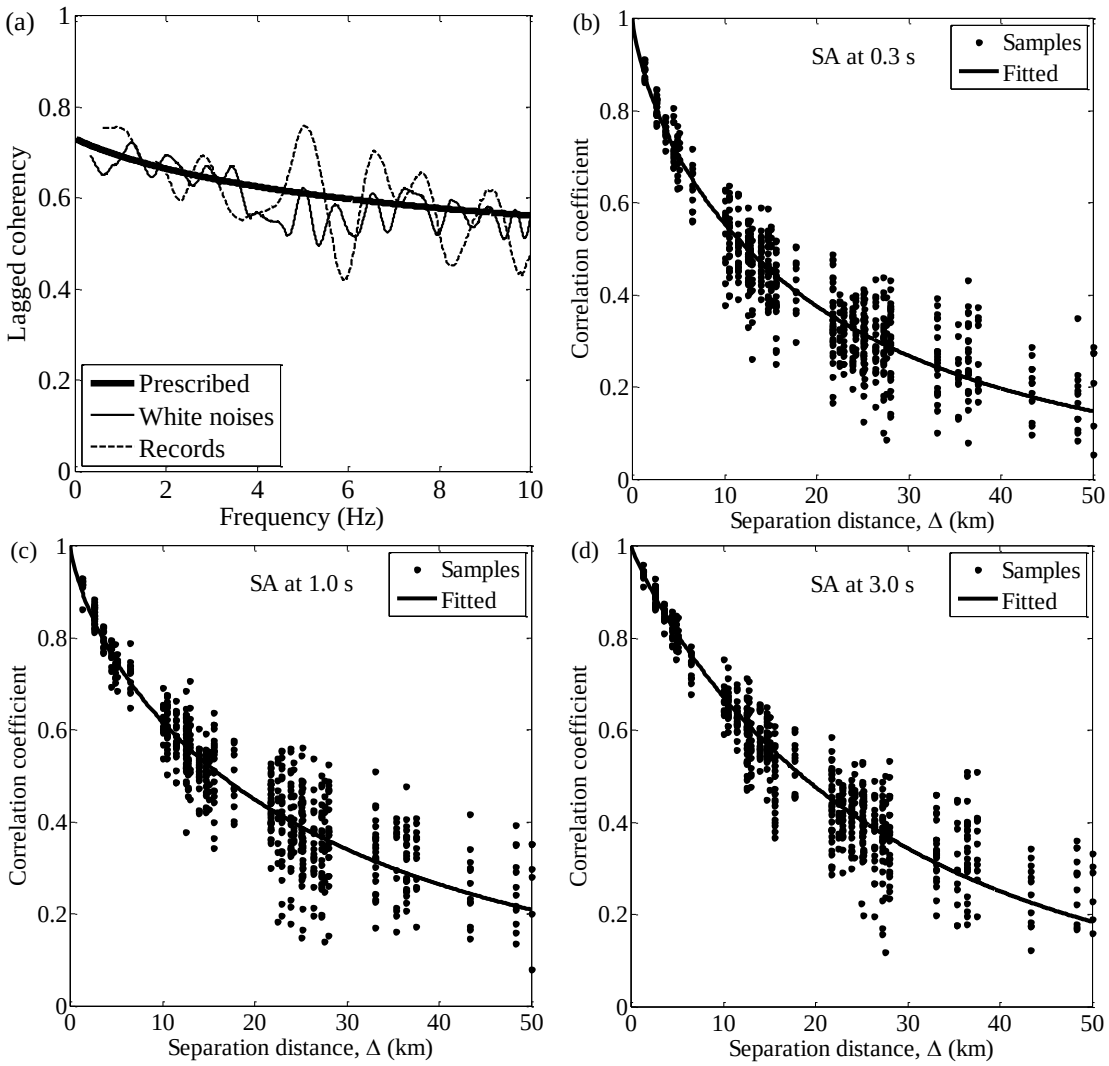


**Figure 4.** Coherency and spatial correlations of the reference case: (a) Lagged coherency between C00 and O25 ($\Delta$ = 25 km) of one simulation cycle; (b), (c) and (d) Spatial correlation coefficients of SAs at 0.3 s, 1.0 s and 3.0 s and their fitted curve based on 100 simulation cycles.

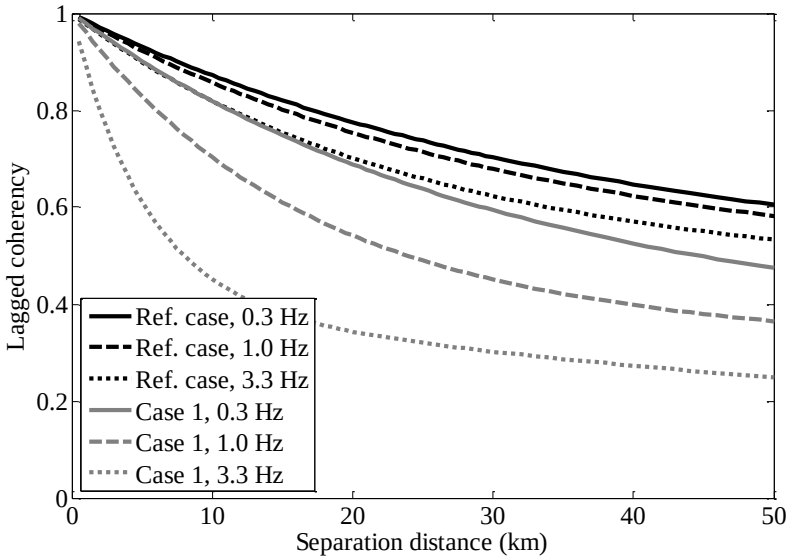


**Figure 5.** Comparison of coherency function used in Case 1 to that of the reference case.

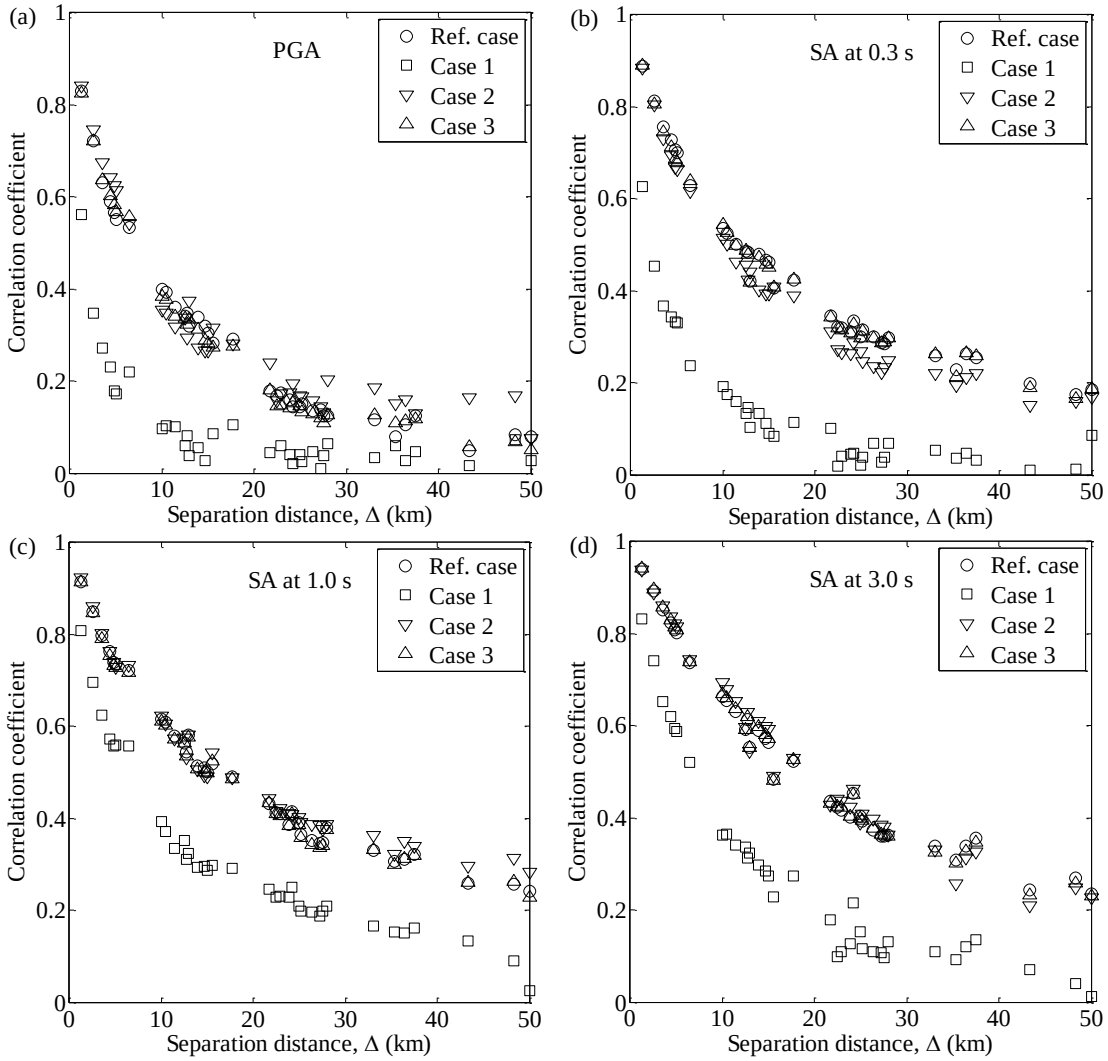


**Figure 6.** Comparison of spatial correlation coefficients (based on 100 simulation cycles) of: (a) PGA; (b) SA at 0.3 s; (c) SA at 1.0 s and (d) SA at 3.0 s.

## 4. CONCLUSIONS AND DISCUSSION

The stochastic point-source method is designed to simulate a record at a station; its direct use cannot simulate records at multiple sites that can reproduce the observed spatial correlation of the PGA or of the SAs from the historical seismic events. To overcome this, we proposed to incorporate the coherency function in the stochastic point-source model to sample the ground motion records at multiple sites. It is shown through numerical examples that the records simulated in such a manner can indeed reproduce the observed trends of the spatial correlation of the PGA and SAs. This is advantageous as the simulated records with sufficient realistic coherency (or spatial correlation) feature can be used to assess risk of a group of buildings or a structure with multiple supports subjected seismic scenario events defined by magnitude and the source to the site distance.

A further scrutiny of the proposed procedure to simulate coherent records may be required since it was observed that the inclusion of coherency alone may not be sufficient to reproduce the observed spatial correlation. Preliminary results show that the consideration of the coherency and the uncertainties of spatially correlated Fourier amplitude spectrum could reproduce the observed spatial correlations. Such an analysis results is to be reported in a near future. Also, the proposal in this study should be extended to the stochastic finite-fault model in order to simulate records with prescribed target spatially coherency and correlation.

**AKCNOWLEDGEMENT**

The financial support received from the Natural Science and Engineering Research Council of Canada and the University of Western Ontario is gratefully acknowledged. One of the authors (T.J. Liu) gratefully acknowledges the support of the China Scholarship Council (No. 2009612007).

**REFERENCES**

Abrahamson, N. A., Schneider, J. F. and Stepp, J. C. (1991). Spatial coherency of shear waves from the Lotung, Taiwan large-scale seismic test. *Structural Safety*, **10**, 145-162.

Atkinson, G. M., Assatourians, K., Boore, D. M., Campbell, K., and Motazedian, D. (2009). A guide to differences between stochastic point-source and stochastic finite-fault simulations. *Bull. Seism. Soc. Am.* **99**, 3192-3201.

Atkinson, G. M., and Boore, D. M. (2006). Earthquake Ground-Motion Prediction Equations for Eastern North America. *Bull. Seism. Soc. Am.* **96**, 2181-2205.

Bolt, B. A., Loh, C. H., Penzien, J., Tsai, Y. B. and Yeh, Y. T. (1982). Preliminary report on the SMART-1 strong motion array in Taiwan, Earthquake Engineering Research Center Report No. UCB/EERC-82/13. University of California, Berkeley, CA.

Boore, D. M. (2003). Simulation of ground motion using the stochastic method. *Pure appl. Geophys.* **160**, 635-676.

Boore, D. M. (1983). Stochastic simulation of high-frequency groundmotions based on seismological models of the radiated spectra. *Bull. Seism. Soc. Am.* **73**, 1865-1894.

Boore, D. M., Gibbs, J. F., Joyner, W. B., Tinsley, J. C., and Ponti, D. J. (2003). Estimated ground motion from the 1994 Northridge, California, earthquake at the site of the Interstate 10 and La Cienega boulevard bridge collapsed, west Los Angeles, California. *Bull. Seism. Soc. Am.* **93**, 2737-2751.

Brillinger, D.R. (1981). Time Series, Data Analysis and Theory. McGraw-Hill, Inc., New York, NY.

Bycroft, G. N. (1980). El Centro, California differential ground motion array. USGS Open- File Report 80-919, U.S. Geological Survey, Denver, CO.

Der Kiureghian, A. (1996). A coherency model for spatially varying ground motions. *Earthquake Eng. Struct. Dynam.* **25**, 99-111.

Kawakami, H., and Mogi, H. (2003). Analyzing spatial intraevent variability of peak ground accelerations as a function of separation distance. *Bull. Seism. Soc. Am.* **93**, 1079-1090.

Jayaram, N., and Baker, J. W. (2009). Correlation model for spatially distributed ground-motion intensities. *Earthq. Eng. Struct. Dynam.* **38**, 1687-1708.

Goda, K., and Hong, H. P. (2008a). Spatial correlation of peak ground motions and response spectra. *Bull. Seism. Soc. Am.* **98**, 354-365.

Goda, K., and Hong, H. P. (2008b). Estimation of seismic loss for spatially distributed buildings. *Earthquake Spectra* **24**(4), 889-910.

Goda, K., and Atkinson, G. M. (2009). Probabilistic characterization of spatially correlated response spectra for earthquakes in Japan. *Bull. Seism. Soc. Am.* **99**, 3003-3020.

Goda, K., and Atkinson, G. M. (2010). Intraevent spatial correlation of ground-motion parameters using SK-net data. *Bull. Seism. Soc. Am.* **100**, 3055-3067.

Hao, H., Oliveira, C.S., and Penzien, J. (1989). Multiple-station ground motion processing and simulation based on SMART-1 array data. *Nucl. Eng. Des.* **111**, 293-310.

Harichandran, R. S., Hawwari, A., and Sweiden, B. N. (1996). Response of long-span bridges to spatially varying ground motion. *Journal of Structural Engineering*, **122**(5), 476-84.

Harichandran R.S., and Vanmarcke E. H. (1986). Stochastic variation of earthquake ground motion in space and time. *J. Eng. Mech.*, **112**, 154-174.

Liu, T. J., Atkinson, G. M., Hong, H. P., and Assatourians, K. (2012). Intraevent Spatial Correlation Characteristics of Stochastic Finite-Fault Simulations. *Bull. Seism. Soc. Am.*, in press.

Motazedian, D., and Atkinson, G. M. (2005). Stochastic finite-fault modeling based on a dynamic corner frequency. *Bull. Seism. Soc. Am.* **95**, 995-1010.

Samaras, E., Shinozuka, M., and Tsurui, A. (1985). ARMA representation of random processes. *J. Eng. Mech.* **111**(3), 449-461.

Wang, M., and Takada, T. (2005). Macrospatial correlation model of seismic ground motions. *Earthq. Spectra* **21**, 1137-1156.

Zerva, A. (1991). Effect of spatial variability and propagation of seismic ground motions on the response of multiply supported structures. *Probabilistic Engineering Mechanics*, **6**,212-21.

Zerva, A. (2009). Spatial variation of seismic ground motions: modeling and engineering applications. CRC Press, Taylor & Francis Group.